



HAL
open science

Photocatalytic, self-cleaning and antibacterial properties of Cu(II) doped TiO₂

Burak Yuzer, Muhammed Iberia Aydin, Ahmet Hilmi Con, Hatice Inan, Safiye Can, Huseyin Selcuk, Yassine Kadmi

► To cite this version:

Burak Yuzer, Muhammed Iberia Aydin, Ahmet Hilmi Con, Hatice Inan, Safiye Can, et al.. Photocatalytic, self-cleaning and antibacterial properties of Cu(II) doped TiO₂. *Journal of Environmental Management*, 2022, 302, pp.114023. 10.1016/j.jenvman.2021.114023 . hal-03636835

HAL Id: hal-03636835

<https://hal.science/hal-03636835v1>

Submitted on 5 Jan 2024

HAL is a multi-disciplinary open access archive for the deposit and dissemination of scientific research documents, whether they are published or not. The documents may come from teaching and research institutions in France or abroad, or from public or private research centers.

L'archive ouverte pluridisciplinaire **HAL**, est destinée au dépôt et à la diffusion de documents scientifiques de niveau recherche, publiés ou non, émanant des établissements d'enseignement et de recherche français ou étrangers, des laboratoires publics ou privés.



Distributed under a Creative Commons Attribution - NonCommercial 4.0 International License

1 **Photocatalytic, self-cleaning and antibacterial properties**
2 **of Cu(II) Doped TiO₂**

3 Burak Yuzer¹, Muhammed Iberia Aydın¹, Ahmet Hilmi Con², Hatice Inan³, Safiye Can¹,
4 Huseyin Selcuk¹, Yassine Kadmi^{4,5*}

5 ¹*Department of Environmental Engineering, Engineering Faculty, Istanbul University-Cerrahpasa,*
6 *Istanbul, Turkey*

7 ²*Department of Food Engineering, Engineering Faculty, Ondokuz Mayıs University, 19 Mayıs*
8 *University, Samsun, Turkey*

9 ³*Department of Environmental Engineering, Gebze Technical University, Gebze, Kocaeli, Turkey*

10 ⁴*LASIRE CNRS UMR 8516, Université Lille, Sciences et Technologies, Villeneuve d'Ascq*
11 *Cedex 59655, France*

12 ⁵*Université d'Artois, IUT de Béthune, 62400, Béthune, France*

13 * *Corresponding authors: e-mail: yassine.kadmi@univ-lille.fr*

14

15 **Abstract**

16 In the study, sol-gel based TiO₂ nanoparticles (NPs) were doped by Cu(II), and the surface of
17 cotton fabric was coated with Cu-doped TiO₂ NPs to develop self-cleaning and antibacterial
18 properties. Coffee stains were introduced on the modified cotton fabric and under suntest
19 illumination; a decrease in the color of coffee stain was followed over time via K/S value to
20 determine self-cleaning performance. The photocurrent in a photoelectrocatalytic reactor was
21 measured to evaluate the photocatalytic effect of Cu(II) doping. TiO₂ NPs showed self-
22 cleaning and antibacterial effects under UV-illuminated conditions. However, no effects were
23 observed under dark (non-illuminated) conditions. The modified textiles with Cu(II) doped
24 TiO₂ NPs showed antibacterial activity against E. coli under light and dark conditions. Under
25 the 2 hr illumination period, fluctuating color changes were observed on the raw cotton fabric,
26 and stains remained on the fabric while 78% and 100% color removals were achieved in the
27 cotton fabrics coated by Cu doped TiO₂ NPs in one hr and two hrs, respectively.

28

29

30 **Keywords:** Cotton fabric, copper doping, Titanium dioxide NPs, self-cleaning, antibacterial
31 activity, photocatalytic effect

32

33 **1. Introduction**

34 The textile industry has focused on nano-technological materials and production
35 systems because of their environmentally friendly and harmless properties. The development
36 of self-cleaning (Liang et al., 2018), antibacterial (Mishra and Butola, 2017), and UV-
37 blocking (Pakdel et al., 2020) ecological nano-textiles with no adverse effects on the
38 environment and human health during production and consumption have gained importance in
39 recent years. Pakdel et al. (2020) have coated cotton fabric by using TiO₂ and hollow glass
40 microspheres to impart thermal insulation, flame retardancy, acoustic performance, UV
41 protection, and mechanical properties. El-Naggar et al. (2016) have studied the antibacterial
42 properties of TiO₂ NPs coated on the cotton fabrics, and they achieved 95% bacterial
43 reduction even after 20 washing cycles. Semiconductor NPs are frequently used to impart
44 these properties to materials.

45 TiO₂ is one of the most studied materials due to its low cost, non-toxic nature,
46 chemical and physical stability, and the oxidation/reduction potential to remove organics
47 (Saad et al., 2016; Zhang et al., 2019). Also, TiO₂ has a bandgap energy of 3.2 eV, and the
48 quantum efficiency of TiO₂ is relatively low under sunlight. The photocatalytic performance
49 of TiO₂ depends on the optical, morphological, and structural properties of TiO₂ (Daghrir et
50 al., 2013; Khaki et al., 2017; Unwiset et al., 2018). The anatase phase of the TiO₂ is known
51 for its high photoactivity, among other phases (Saad et al., 2016). However, high-temperature
52 calcination (300-1000°C) is required to obtain highly photoreactive crystalline phases, which
53 is unsuitable for textile applications (Mathew et al., 2018). Alternative coating methods to
54 calcination have been investigated to overcome this problem, and promising results have been
55 gathered (Doganli et al., 2016; Li et al., 2018).

56 To improve the photocatalytic efficiency of TiO₂, it is necessary to decrease the
57 recombination rate of the photoexcited electron-hole pair. In recent years, many different
58 methods have been progressed to overcome these challenges, such as optimizing powders
59 morphology, doping TiO₂ with metals, and preparing TiO₂ composites (Etacheri et al., 2015).
60 Adding metals or metal oxides into the bulk of a photocatalyst prevents the recombination of
61 excited electron-hole pair, may reduce the bandgap energy, and enhances the photocatalyst's
62 performance (Etacheri et al., 2015; Pelaez et al., 2012). Furthermore, the modification of TiO₂
63 by doping transition metals like Cr, Zn, Ag, and Cu can extend the UV absorption threshold
64 of TiO₂ towards the visible region (Khaki et al., 2017; Mathew et al., 2018; Yoong et al.,
65 2009). The sol-gel method is a facile, reproducible, low-cost, and low-temperature chemical
66 process to prepare doped and nondoped TiO₂ NPs (Casagrande et al., 2018). Particle size
67 distribution, surface area, morphology and the crystallinity of the product powder, the
68 thickness of the film, and phase content can be controlled by solution variables such as
69 precursor's nature, water-to-titanium molar ratio, pH of the prepared solution, dipping time,
70 etc. (Sayilkan et al., 2005; Shan et al., 2010).

71 In addition to TiO₂ NPs, various metal oxide NPs have also been used to impart
72 antibacterial and self-cleaning properties to fabrics. Kumbhakar et al. (2018) have synthesized
73 reduced graphene oxide, and ZnO nanocomposites to impart self-cleaning properties to the
74 cotton fabric and had achieved 91% methylene blue removal from fabric in 60 min under
75 UV-vis light irradiation. Another study reported by Ahmad et al. (2019) coated cotton fabric
76 with Reactive Blue-25 (RB-25)/TiO₂ using the sol-gel method, and 91% degradation of
77 Rhodamine B dye was achieved. Tahmasebizad et al. (2020) have investigated the
78 antibacterial behavior of TiO₂ co-doped with copper and nitrogen via the sol-gel method and
79 reported that co-doping of TiO₂ enhanced the photocatalytic activity and antibacterial
80 characteristics of the samples. Also, Komaraiah et al. (2019) have synthesized Fe-doped and

81 non-doped TiO₂ NPs using the sol-gel method. They reported that the Fe-doped TiO₂ NPs
82 showed more catalytic activity compared to non-doped TiO₂. Another study investigated the
83 antibacterial and self-cleaning properties of Mn-doped TiO₂ NPs that were deposited on the
84 cotton fabric (Zahid et al., 2018). It has been reported that 100% reduction of *Staphylococcus*
85 *aureus* (Gram-positive) and *Klebsiella pneumoniae* (Gram-negative) populations were
86 achieved within 120 min under sunlight. Also, complete degradation of a methylene blue
87 (MB) dye adsorbed on the fabric's surface was accomplished.

88 Altering the structural properties of TiO₂ by metal doping may modify its
89 biocompatibility. Several studies have been published previously on the effect of different
90 metal dopants on the bioactivity of TiO₂ (Aich et al., 2016; Mathew et al., 2018; Rao et al.,
91 2018). Among many metals mentioned above, copper-based compounds exhibit superior
92 effects on the photocatalytic and antibacterial performance of TiO₂ (Estekhraji and Amiri,
93 2017; Leyland et al., 2016; Unwiset et al., 2018). Furthermore, copper-modified TiO₂ exhibits
94 antibacterial properties in the dark without UV. However, there is limited information about
95 the effect of Cu doping on antibacterial and self-cleaning textile products. To our knowledge,
96 there is only one work about copper modified textile surface done by Ibrahim et al. (2019),
97 who worked on self-cleaning, UV protection, and the antibacterial effect with Cu₂O/TiO₂.

98 In this study, TiO₂ was doped with Cu(II) by the sol-gel method, and for the first time,
99 photoelectrocatalytic (PEC) properties have been associated with self-cleaning and
100 antibacterial properties. A cotton textile fabric was coated to provide self-cleaning and
101 antibacterial properties. The performance of the modified cotton textile fabric was presented
102 under both dark and UV-illuminated conditions.

103

104

105 **2. Experimental methods and materials**

106 *2.1. Synthesis of Cu-doped TiO₂ and coating of cotton fabric*

107 The sol-gel method was used to synthesize TiO₂ NPs, as described in the previous
108 study (Chehade et al., 2018). To prepare the sol-gel solution, 25 ml of TTIP (Aldrich; 97%)
109 and 5 ml of acetic acid were added to 500 ml of distilled water. Then, 3.5 ml of HNO₃ was
110 added, and the resulting mixture was heated at 80 °C for 30 minutes. The formed TiO₂ colloid
111 was mixed with a magnetic stirrer for 2 hours. The prepared solution was dialyzed against a
112 pH of 2.5 aqueous HCl by using Spectra/PorDialysis membrane tubing (MWCO: 6–8 kD) to
113 increase the pH of the sol-gel solution above 2 to prevent recombination of TiO₂ NPs. The
114 dialyzing solution was replaced frequently (Foorginezhad and Zerafat, 2019). Then, the
115 copper solution was prepared by adding Copper(II) sulfate pentahydrate (Sigma-Aldrich
116 ReagentPlus[®], ≥99% CAS #: 7758-98-7) into sol-gel solution dropwise as a Cu precursor, and
117 an appropriate amount of solution that gives Cu(II)/solution ratio of 0.2%, 0.5%, 1%, 3%, and
118 5.5% by mass was mixed with the prepared TiO₂ solution.

119 Commercial cotton gray fabric (100%) was supplied from the manufacturer, and the
120 fabric was scoured with non-ionic detergent to get rid of any possible wax, grease, simple
121 stains, and other compounds from the fabric surface before the coating process. After
122 pretreatment, the cotton fabric was cut into small pieces (5 cm×5 cm). TiO₂ NPs were
123 deposited on the prepared cotton fabrics by using the dip-coating process. The dip-coating
124 device set to the 2.5 mm/sec withdrawal rate, 5-999 mm/min varied movement speed,
125 430 mm of working range. The number of moves was adjusted to 100. Then, the cotton
126 fabrics were rinsed and dried at room temperature. Finally, textile fabrics were subjected to
127 heat treatment at 100 °C to activate the films.

128

129 *2.2. Characterization of TiO₂ nanoparticles*

130 Concentrated sulfuric acid was used to decompose 10 mg of coated cotton fabric
131 samples. After the decomposition process, the solution was neutralized to analyze the
132 presence and amount of TiO₂ NPs. The particle size distribution of TiO₂ NPs was measured
133 using a Zetasizer (Malvern Nano ZS90, at room temperature, water refraction index of 1.33;
134 viscosity of 0.8872; and pH 4–8). FEI-Philips XL30 Environmental Scanning Electron
135 Microscope (SEM) was used to take images of the coated NPs on the fabric.

136 *2.3 Antimicrobial activity test*

137 The antibacterial properties of the coated textile materials were tested by using
138 *Staphylococcus aureus* ATCC 29213 and *Escherichia coli* ATCC 25922 following the
139 AATCC Test Method (Adi B. Chehna, Ann Laidlaw, Leander B. Ricard, 2015). Stock
140 cultures of the bacteria were kept in a Nutrient Agar (NA). Before each activity test, bacteria
141 were incubated at $37 \pm 0.1^\circ\text{C}$ for 24 h in the nutrient broth. The concentration of culture
142 suspensions was adjusted to 10⁶ CFU/mL (colony-forming units per milliliter) via 0.5
143 McFarland turbidity standard tubes. Cotton fabric samples having a size of $8 \pm 0.1 \text{ cm}^2$ (2 cm
144 x 4 cm) were utilized in all experiments. After adding the inoculum (100 mL), both coated
145 and uncoated fabric samples were illuminated with 500 W at 35°C and in the solar simulator
146 equipment (ATLAS SUNTEST). Then, the cotton fabrics were shaken in nutrient broth
147 (25 mL) for three minutes. Parallel seeding was made by drip method from 4 consecutive
148 dilutions into Nutrient Agar medium, and after incubation of petri dishes at $37 \pm 0.2^\circ\text{C}$ for 24–
149 48 hours, all growing colonies were counted. All experiments were conducted in duplicate.
150 The number of bacteria in each sample (CFU/cm² per fabric) was monitored to assess the
151 antibacterial activity in cotton fabrics. Uncoated and coated samples were subjected to an
152 antibacterial activity test under UV light exposure.

153 2.4 Assessment of coffee stain degradation for self-cleaning activity

154 Since coffee stains are the leading stains that occur in real life, the fabrics are stained
155 with coffee. The coffee stains were photocatalytically degraded to evaluate the self-cleaning
156 activity of cotton fabrics (coffee bag, 2 g/200 mL brewed at 80°C distilled water for 2 min).
157 Uncoated (control) and TiO₂-coated white fabric samples were disintegrated into small pieces
158 (5 cm × 5 cm). The samples were immersed in the hot coffee until the coffee was fully
159 absorbed throughout the fabric. Afterward, the samples were rinsed with clean water and then
160 exposed to light in the SUNTEST solar simulator. The color of coated and uncoated fabric
161 samples was then measured using the color-measuring device (Data Color 600 Dual-Beam
162 Spectrophotometer), and the color differences between uncoated and coated samples were
163 calculated. The self-cleaning activity test of cotton fabric was performed, as described in our
164 previous study (Doganli et al., 2016). The color difference values for each fabric sample were
165 accepted as self-cleaning efficiency of the samples, and it was quantified with the terms of
166 delta E (dE) and K/S. The dE and K/S values of measured samples were obtained directly
167 from the color measurement device. Components of the dE color measurement system are
168 positioned in a three-dimensional space. Those components are lightness of color ($L^* = 0$
169 yielded black and $L^* = 100$ indicated diffuse white), the position of color in color space
170 between green and red/magenta (a^* , negative values indicated green color, while positive
171 values indicated red/magenta), and position of color in color space between blue and yellow
172 (b^* , negative values indicated blue and positive values indicated yellow). Color value
173 differences between sample fabric and reference fabric for L^* , a^* , and b^* parameters are
174 calculated using equations (1)–(4);

175 $dL^* = L^*_{sample} - L^*_{reference}$ (1)

176 $da^* = a^*_{sample} - a^*_{reference}$ (2)

177 $db^* = b_{sample}^* - b_{reference}^*$ (3)

178 Total color difference, (dE), is calculated from dL*, da*, and db* as follows:

179 $dE = [(dL^*)^2 + (da^*)^2 + (db^*)^2]^{1/2}$ (4)

180 K/S value is a ratio of light absorption (K) and light scattering (S) characteristics of color, and
181 it is calculated depending on spectral reflectance (R in %) of the sample as it is given in
182 equation (5):

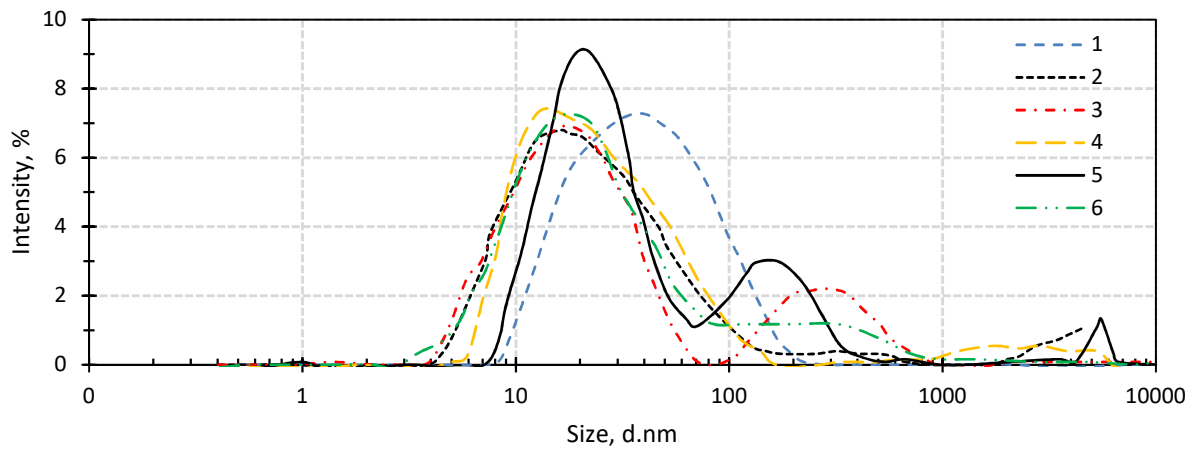
183 $K/S = (1 - 0.01R)^2 / 2(0.01R)$ (5)

184 **3. Results**

185 *3.1 The effect of Cu(II) adding on the particle size distribution of TiO₂ NPs*

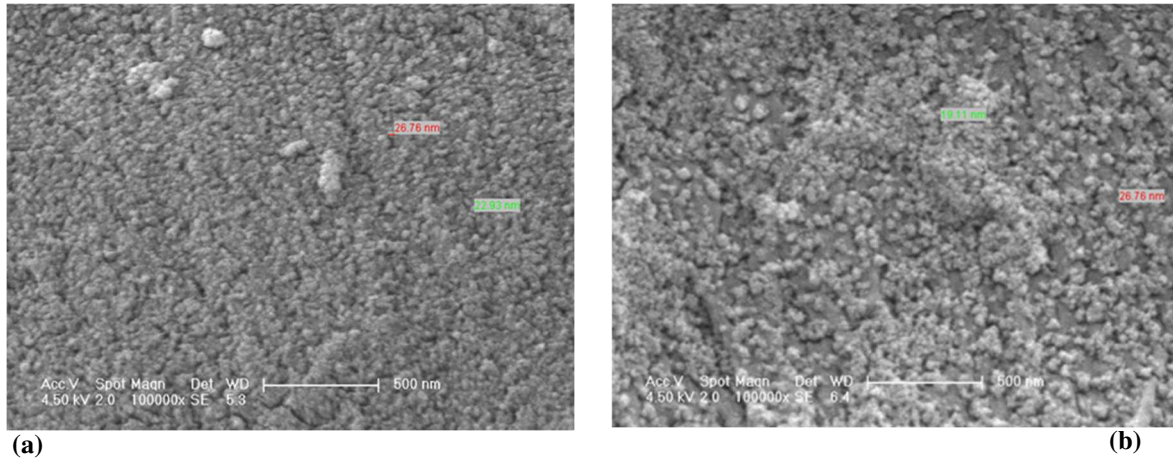
186 Film thickness, morphology, size, porosity, optical and electronic structure of the NPs
187 depend on production technique and further coating processing. These parameters determine
188 surface conditions for the formation of products and light conversion for treatment
189 technologies. The advantages of the sol-gel method are good homogeneity, ease of
190 composition control, low processing temperature, large area coatings, low equipment cost,
191 and excellent photocatalytic properties (Akpan and Hameed, 2010; Sayilkan et al., 2005).
192 (Jonidi Jafari and Moslemzadeh, 2020) have reviewed the literature to monitor the effect of
193 synthesis methods of Fe-doped TiO₂ NPs for photocatalytic processes under UV-visible light,
194 and it has been reported that the crystal sizes range from 5 to 25 nm in many studies. On the
195 other hand, (Komaraiah et al., 2019) reported that the crystallite size of TiO₂ reduced from
196 9.64 nm to 7 nm with Fe doping. In the present study, the sol-gel method was applied to
197 prepare TiO₂ and Cu-doped TiO₂ NPs. Figure 1 shows the size distribution of 0-10% Cu(II)
198 doped TiO₂ NPs. Without doping, the average size distribution of the TiO₂ NPs was found to

199 be 28 nm. No significant change was observed in particle size with Cu(II) doping, and the
200 average size distribution was found in the range of 18-32 nm.



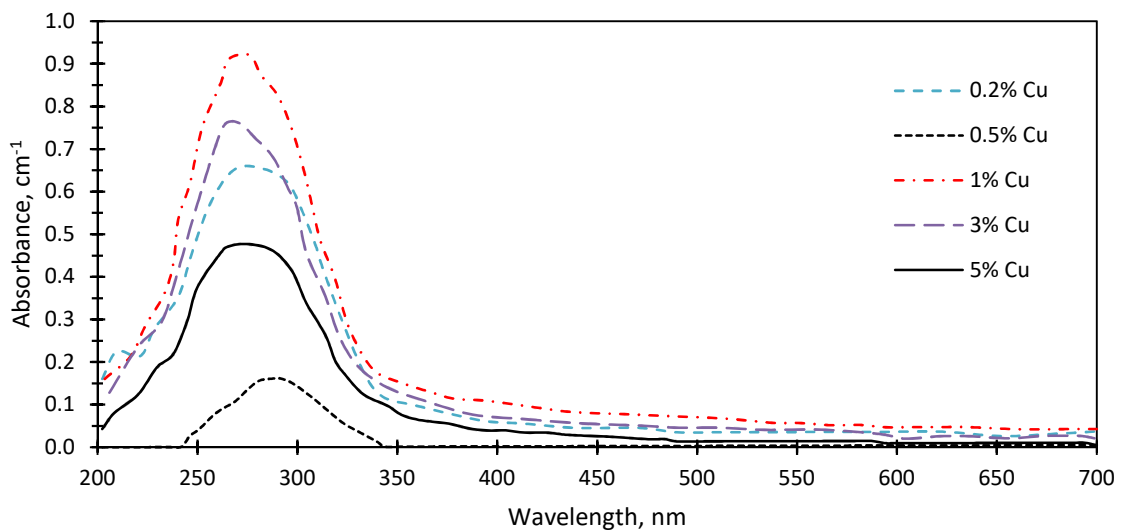
201
202 **Figure 1.** The particle size distribution of Cu-doped sol-gel (Cu ratio in sol-gel; 1: 0.2%, 2:
203 0.5%, 3: 1%, 4: 3%, 5: 5%, 6: nondoped)

204 Increasing the zeta potential by metal doping is important for the adsorption and then the
205 deactivation of negatively charged bacteria on the surface of textile fabrics (Slavin et al.,
206 2017). The zeta potential of TiO₂ NPs was measured after each doping and was observed to
207 increase with Cu(II) doping. The zeta potential of non-doped TiO₂ was 6.0, and it reached
208 6.62 with 10% Cu(II) doping. It is reported that Cu(II) may shift the UV absorbance range of
209 TiO₂ to the visible range (Mathew et al., 2018; Yoong et al., 2009). The images of
210 immobilized Cu-doped and non-doped NPs on the cotton fabric are given in Figure 2. The
211 Cu-doped TiO₂ NPs are clearly seen in Figure 2 (a), and the size of the doped NPs was
212 measured as 22.9 – 26.7 nm.



213 **Figure 2.** The SEM images for (a) 5% Cu-doped TiO₂ and (b) non-doped TiO₂ NPs.

214 UV-Vis absorbance spectra show that Cu(II) does not change the max absorbance range of
 215 TiO₂, but it allows TiO₂ to absorb visible light (Fig. 3).



216 **Figure 3.** The absorbance values for different doping ratios of Cu-doped TiO₂ NPs in the sol-
 217 gel solution prepared at 100 °C.
 218

219 Powdered TiO₂ NPs obtained at 100 °C before and after Cu(II) doping are shown in Figure 4.
 220 The color of commercially available TiO₂ powder is white. Thus, it is just suitable for white
 221 textile fabric. However, in this study, yellowish TiO₂ powder was achieved by Cu(II) doping.
 222 Therefore, this may be an advantage for using TiO₂ for the colored textile fabric.



Figure 4. The images for (a) 5% Cu-doped TiO₂ and (b) non-doped TiO₂ NPs.

3.2. The effect of Cu(II) doping on the photoelectrocatalytic performance of TiO₂ NPs

The photocatalytic chemistry of TiO₂ has been extensively studied over the few decades to understand the fundamentals of photochemical processes. The mechanism of the TiO₂ photocatalytic process is based on the formation of photo-excited electrons and holes. As electrons and holes are generated, many different chain reactions may be initiated, resulting in the formation of strong hydroxyl radicals (OH•) (Fig. 5).

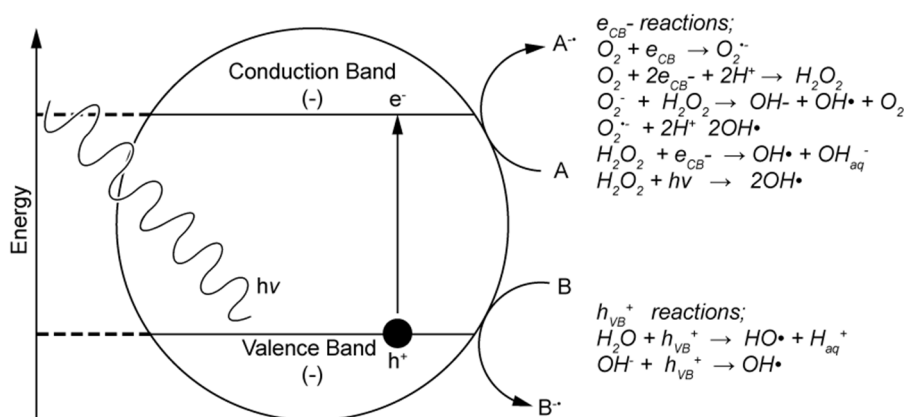
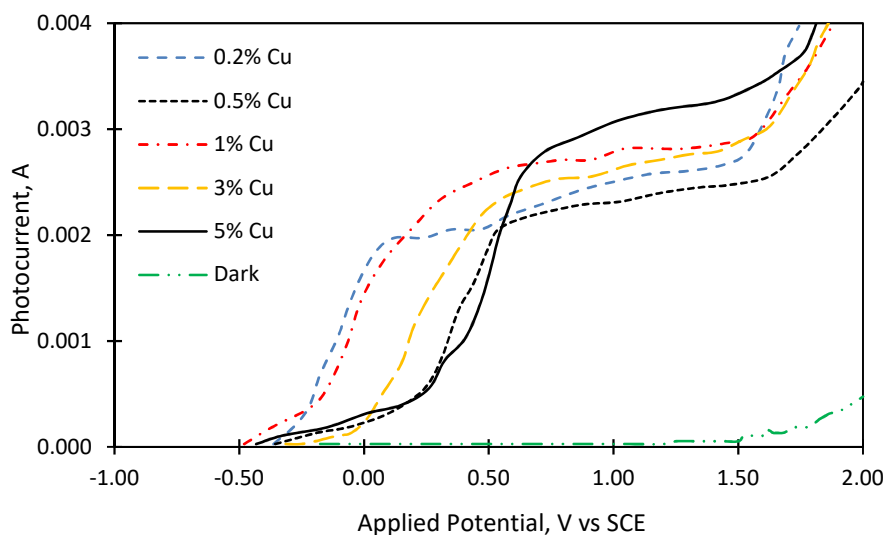


Figure 5. Principles of the photocatalytic process.

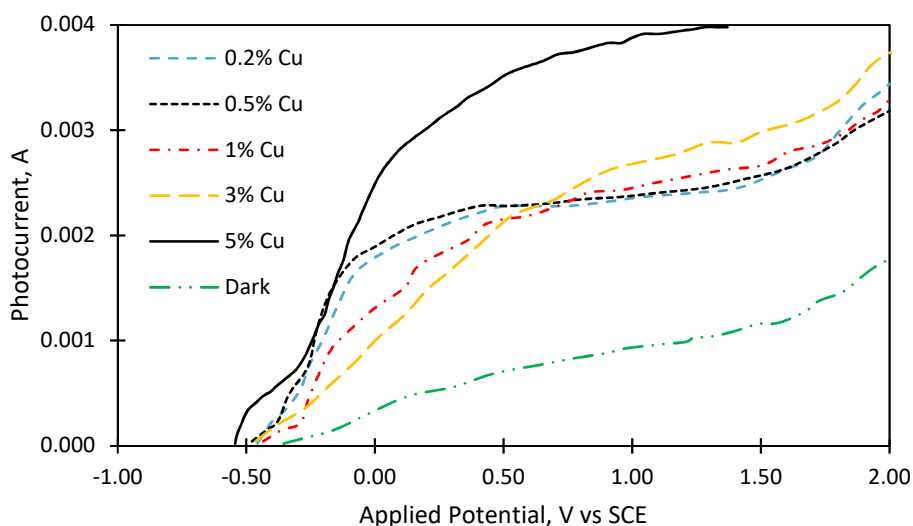
OH• radicals play an important role in removing bacteria, organic and inorganic contaminants (Doganli et al., 2016; Mahmoodi et al., 2006; Moongraksathum et al., 2018). However, in the absence of electron donors or acceptors, electron-hole pairs (e_{CB}^-/h_{VB}^+), have a life span of a few nanoseconds. Recombination of electron-hole pairs must be slowed to enhance photoactivity. One of the current strategies to enhance the photoactivity of TiO₂ is

238 doping TiO₂ with metal and non-metal ions to shift photo-response to the visible spectrum
239 (Cong et al., 2011; Singh et al., 2019). A decrease in photocatalytic activity of TiO₂ is still a
240 disadvantage regarding metal doping methods. The immobilization method determines
241 photocatalytic activity of TiO₂.

242 In recent years, photoelectrochemical (PEC) methods have been widely adopted to
243 measure the photocatalytic performance of novel TiO₂ NPs (Shan et al., 2010; Zhu et al.,
244 2007). In this study, the photocurrent generated in a PEC reactor was used to evaluate the
245 effects of calcination temperature and Cu(II) doping rate on the photocatalytic performance of
246 TiO₂ nanofilms. It is well known that the photoactive phase of TiO₂ can be obtained over
247 300°C. However, in this study, the results showed that the TiO₂ film is active even at 25°C. A
248 1% Cu doping was found to be optimum doping rate at the temperatures of both 400°C and
249 25°C to get max photocurrent (Fig. 6 and Fig. 7).



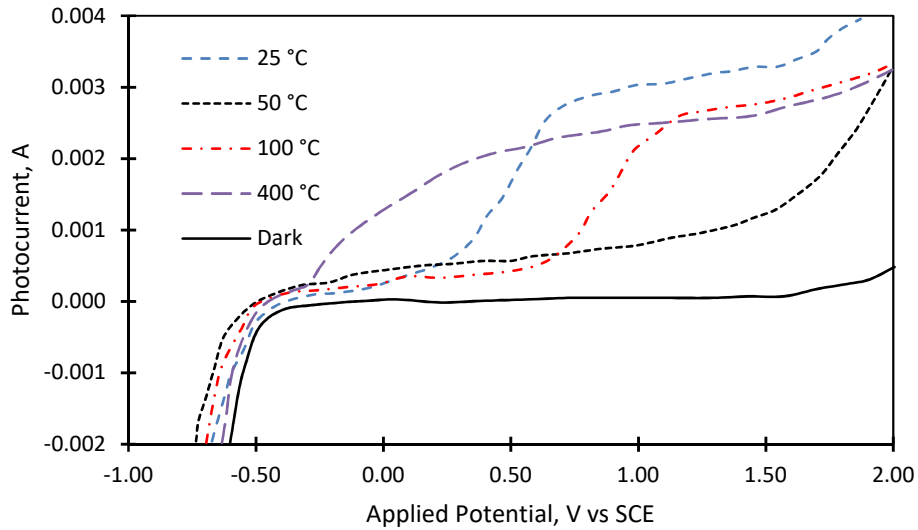
250 **Figure 6.** The photocurrent values for different doping ratios of Cu-doped TiO₂ NPs in the
251 sol-gel solution prepared at 25 °C.
252



253

254 **Figure 7.** The photocurrent values for different doping ratios of Cu-doped TiO₂ NPs in the
 255 sol-gel solution prepared at 400 °C.

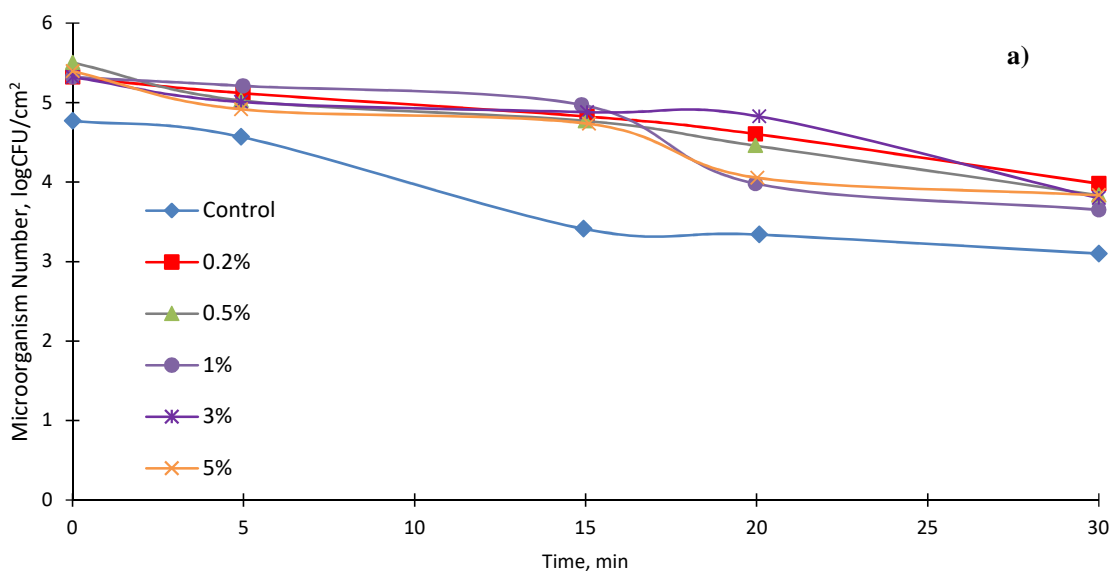
256 A small number of studies show that TiO₂ calcined at low temperature values may
 257 show photocatalytic property (Saad et al., 2016). There are still many gaps to be clarified
 258 about the measurement of anatase and rutile phase in the amorphous phase achieved at low
 259 temperatures. Also, commercially available Degussa P25 consisting of anatase and rutile
 260 mixture is still the best performing photocatalyst (El-Sheikh et al., 2014). Results show that
 261 calcination at a higher temperature just decreased the activation energy of TiO₂ films, but
 262 TiO₂ powder calcined at low-temperature values may be photoactive at higher illumination or
 263 external potential values (Fig. 8).

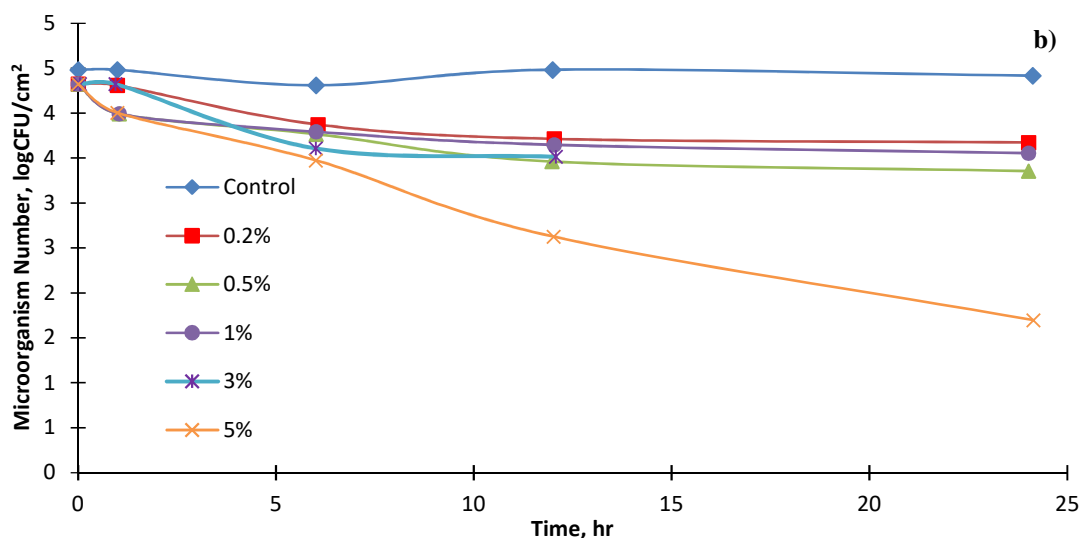


264 **Figure 8.** The Effect of sol-gel temperature on photocurrent (1% Cu-doping).

265 *3.3. Antibacterial properties of Cu doped TiO₂*

266 Results show that TiO₂ and Cu(II)-doped TiO₂ NPs increased the E. coli number on
 267 the textile surface. These results were attributed to the hydrophilic effect of TiO₂ on the cotton
 268 surface. However, the deactivation of E. coli on the raw and modified textiles is almost the
 269 same as initial log CFU decreased from 5.5 to 4 on the modified textile fabrics, while the
 270 initial E. coli number decreased from log 4.8 to log 3.4.





271 **Figure 9.** Antibacterial properties of the doped-TiO₂ NPs: (a) change in the number of
 272 microorganisms by minute and (b) change in the number of microorganisms by the hour.

273 The antibacterial experiments were also performed in the dark. As shown in Figure 9,
 274 even after 25 hours of incubation time under dark conditions, no antibacterial effect was
 275 observed on the non-doped TiO₂ coated cotton fabric while Cu(II) doping clearly exhibits an
 276 antibacterial effect, and a significant antibacterial effect was achieved in the dark at 5% Cu(II)
 277 doping rate.

278 3.4. Self-cleaning Effect

279 Most of the studies in the literature used dye solutions to determine the self-cleaning
 280 performance of the TiO₂ NPs (Shaban et al., 2016; Zahid et al., 2018). However, in this study,
 281 coffee stains were used on the fabrics to represent real-life stains on the clothes. Even
 282 stronger initial color was observed on the 1% Cu(II) doped cotton fabric. However, 78% color
 283 removal was achieved under illumination in one hour, and color disappeared in two hours.
 284 Similar studies were conducted with methylene blue solution. (Zahid et al., 2018) reached
 285 97% methylene blue removal efficiency in ten hours by using Mn-doped TiO₂ NPs, while
 286 (Komaraiah et al., 2019) have reached 96.7 methylene blue removal in four hours with Fe-
 287 doped TiO₂ NPs. The initial color was light on the raw cotton textile. However, some darker

288 color was observed even after a two-hour illumination period. Results reflect that Cu(II)
289 doping may provide TiO₂ NPs not only antibacterial property but also self-cleaning function
290 (Fig. 10).



291 **Figure 10.** Self-cleaning performance of 1% Cu(II) doped TiO₂ calcined at 25 °C.

292 4. Conclusion

293 Under UV illumination, TiO₂ NPs provide textile fabric self-cleaning and antibacterial
294 properties. However, under dark conditions, the TiO₂ coated textile surface may not be
295 antibacterial. Thus, in this study, Cu(II) doping was applied to provide cotton fabric
296 antibacterial function in the dark. The sol-gel based Cu(II) doped TiO₂ NPs were dip-coated
297 on the Ti foil at different temperatures. The photocatalytic performance of the modified films
298 was measured in a PEC reactor by photocurrent measurement. Coffee was used to stain the
299 cotton fabric, and the K/S ratio was observed to determine the self-cleaning performance.
300 Even at 25 °C, photocurrent was achieved at 0.5 V external potential. This means that the film
301 achieved at low temperature values may be active at higher illumination intensities. As
302 expected, a significant antibacterial function was achieved in the dark at the high Cu(II)

303 loading of 5%. Coffee stain removals measured as K/S value improves that even at low-
304 temperature values, sol-gel based Cu(II) doped TiO₂ NPs may exhibit a self-cleaning effect
305 under sunshine illumination provided by solar simulator equipment.

306 **Acknowledgments**

307 The authors would like to thank the Scientific and Technological Research Council of Turkey
308 (TUBITAK) for the research grant 108M211.

309 **Declaration of competing interest**

310 The authors declare that they have no known competing financial interests or personal
311 relationships that could have appeared to influence the work reported in this paper

312

313 **References**

314 Adi B. Chahna, Ann Laidlaw, Leander B. Ricard, A.R.V., 2015. AATCC - Technical Manual,
315 American Association of Textile Chemists and Colorists.

316 Ahmad, I., Kan, C. wai, Yao, Z., 2019. Reactive Blue-25 dye/TiO₂ coated cotton fabrics with
317 self-cleaning and UV blocking properties. *Cellulose* 26, 2821–2832.

318 <https://doi.org/10.1007/s10570-019-02279-2>

319 Aich, S., Mishra, M.K., Sekhar, C., Satapathy, D., Roy, B., 2016. Synthesis of Al-doped Nano
320 Ti-O scaffolds using a hydrothermal route on Titanium foil for biomedical applications.

321 *Mater. Lett.* 178, 135–139. <https://doi.org/10.1016/j.matlet.2016.05.003>

322 Akpan, U.G., Hameed, B.H., 2010. The advancements in sol–gel method of doped-TiO₂
323 photocatalysts. *Appl. Catal. A Gen.* 375, 1–11.

324 <https://doi.org/10.1016/j.apcata.2009.12.023>

325 Casagrande, R.B., Kunst, S.R., Beltrami, L.V.R., Aguzzoli, C., Brandalise, R.N., de Fraga

326 Malfatti, C., 2018. Pretreatment effect of the pure titanium surface on hybrid coating
327 adhesion based on tetraethoxysilane and methyltriethoxysilane. *J. Coatings Technol. Res.*
328 15, 1089–1106. <https://doi.org/10.1007/s11998-017-0035-2>

329 Chehade, G., Demir, M.E., Dincer, I., Yuzeer, B., Selcuk, H., 2018. Experimental investigation
330 and analysis of a new photoelectrochemical reactor for hydrogen production. *Int. J.*
331 *Hydrogen Energy* 43, 12049–12058. <https://doi.org/10.1016/j.ijhydene.2018.04.110>

332 Cong, Y., Li, X., Qin, Y., Dong, Z., Yuan, G., Cui, Z., Lai, X., 2011. Carbon-doped TiO₂
333 coating on multiwalled carbon nanotubes with higher visible light photocatalytic activity.
334 *Appl. Catal. B Environ.* 107, 128–134. <https://doi.org/10.1016/j.apcatb.2011.07.005>

335 Daghrir, R., Drogui, P., Robert, D., 2013. Modified TiO₂ For Environmental Photocatalytic
336 Applications: A Review. *Ind. Eng. Chem. Res.* 52, 3581–3599.
337 <https://doi.org/10.1021/ie303468t>

338 Doganli, G., Yuzeer, B., Aydin, I., Gultekin, T., Con, A.H., Selcuk, H., Palamutcu, S., 2016.
339 Functionalization of cotton fabric with nanosized TiO₂ coating for self-cleaning and
340 antibacterial property enhancement. *J. Coatings Technol. Res.* 13, 257–265.

341 El-Naggar, M.E., Shaheen, T.I., Zaghoul, S., El-Rafie, M.H., Hebeish, A., 2016.
342 Antibacterial Activities and UV Protection of the in Situ Synthesized Titanium Oxide
343 Nanoparticles on Cotton Fabrics. *Ind. Eng. Chem. Res.* 55, 2661–2668.
344 <https://doi.org/10.1021/acs.iecr.5b04315>

345 El-Sheikh, S.M., Zhang, G., El-Hosainy, H.M., Ismail, A.A., O’Shea, K.E., Falaras, P.,
346 Kontos, A.G., Dionysiou, D.D., 2014. High performance sulfur, nitrogen and carbon
347 doped mesoporous anatase–brookite TiO₂ photocatalyst for the removal of microcystin-
348 LR under visible light irradiation. *J. Hazard. Mater.* 280, 723–733.

349 <https://doi.org/10.1016/j.jhazmat.2014.08.038>

350 Estekhraji, S.A.Z., Amiri, S., 2017. Sol–gel preparation and characterization of antibacterial
351 and self-cleaning hybrid nanocomposite coatings. *J. Coatings Technol. Res.* 14, 1335–
352 1343. <https://doi.org/10.1007/s11998-017-9932-7>

353 Etacheri, V., Di Valentin, C., Schneider, J., Bahnemann, D., Pillai, S.C., 2015. Visible-light
354 activation of TiO₂ photocatalysts: Advances in theory and experiments. *J. Photochem.*
355 *Photobiol. C Photochem. Rev.* 25, 1–29.
356 <https://doi.org/10.1016/j.jphotochemrev.2015.08.003>

357 Foorginezhad, S., Zerafat, M.M., 2019. Fabrication of stable fluorine-free superhydrophobic
358 fabrics for anti-adhesion and self-cleaning properties. *Appl. Surf. Sci.* 464, 458–471.
359 <https://doi.org/10.1016/j.apsusc.2018.09.058>

360 Ibrahim, M.M., Mezni, A., El-Sheshtawy, H.S., Abu Zaid, A.A., Alsawat, M., El-Shafi, N.,
361 Ahmed, S.I., Shaltout, A.A., Amin, M.A., Kumeria, T., Altalhi, T., 2019. Direct Z-
362 scheme of Cu₂O/TiO₂ enhanced self-cleaning, antibacterial activity, and UV protection
363 of cotton fiber under sunlight. *Appl. Surf. Sci.* 479, 953–962.
364 <https://doi.org/https://doi.org/10.1016/j.apsusc.2019.02.169>

365 Jonidi Jafari, A., Moslemzadeh, M., 2020. Synthesis of Fe-Doped TiO₂ for Photocatalytic
366 Processes under UV-Visible Light: Effect of Preparation Methods on Crystal Size—A
367 Systematic Review Study. *Comments Inorg. Chem.* 40, 327–346.
368 <https://doi.org/10.1080/02603594.2020.1821674>

369 Khaki, M.R.D., Shafeeyan, M.S., Raman, A.A.A., Daud, W.M.A.W., 2017. Application of
370 doped photocatalysts for organic pollutant degradation - A review. *J. Environ. Manage.*
371 198, 78–94. <https://doi.org/10.1016/j.jenvman.2017.04.099>

372 Komaraiah, D., Radha, E., Sivakumar, J., Ramana Reddy, M.V., Sayanna, R., 2019.
373 Structural, optical properties and photocatalytic activity of Fe³⁺ doped TiO₂ thin films
374 deposited by sol-gel spin coating. *Surfaces and Interfaces* 17, 100368.
375 <https://doi.org/10.1016/j.surfin.2019.100368>

376 Kumbhakar, Partha, Pramanik, A., Biswas, S., Kole, A.K., Sarkar, R., Kumbhakar, Pathik,
377 2018. In-situ synthesis of rGO-ZnO nanocomposite for demonstration of sunlight driven
378 enhanced photocatalytic and self-cleaning of organic dyes and tea stains of cotton
379 fabrics. *J. Hazard. Mater.* 360, 193–203. <https://doi.org/10.1016/j.jhazmat.2018.07.103>

380 Leyland, N.S., Podporska-Carroll, J., Browne, J., Hinder, S.J., Quilty, B., Pillai, S.C., 2016.
381 Highly Efficient F, Cu doped TiO₂ anti-bacterial visible light active photocatalytic
382 coatings to combat hospital-acquired infections. *Sci. Rep.* 6, 24770.
383 <https://doi.org/10.1038/srep24770>

384 Li, Z., Dong, Y., Li, B., Wang, P., Chen, Z., Bian, L., 2018. Creation of self-cleaning
385 polyester fabric with TiO₂ nanoparticles via a simple exhaustion process: Conditions
386 optimization and stain decomposition pathway. *Mater. Des.* 140, 366–375.
387 <https://doi.org/10.1016/j.matdes.2017.12.014>

388 Liang, Y., Sun, S., Deng, T., Ding, H., Chen, W., Chen, Y., 2018. The Preparation of TiO₂
389 Film by the Sol-Gel Method and Evaluation of Its Self-Cleaning Property. *Materials*
390 (Basel). 11, 450. <https://doi.org/10.3390/ma11030450>

391 Mahmoodi, N.M., Arami, M., Limaee, N.Y., Tabrizi, N.S., 2006. Kinetics of heterogeneous
392 photocatalytic degradation of reactive dyes in an immobilized TiO₂ photocatalytic
393 reactor. *J. Colloid Interface Sci.* 295, 159–164. <https://doi.org/10.1016/j.jcis.2005.08.007>

394 Mathew, S., Ganguly, P., Rhatigan, S., Kumaravel, V., Byrne, C., Hinder, S., Bartlett, J.,

395 Nolan, M., Pillai, S., 2018. Cu-Doped TiO₂: Visible Light Assisted Photocatalytic
396 Antimicrobial Activity. *Appl. Sci.* 8, 2067. <https://doi.org/10.3390/app8112067>

397 Mishra, A., Butola, B.S., 2017. Deposition of Ag doped TiO₂ on cotton fabric for wash
398 durable UV protective and antibacterial properties at very low silver concentration.
399 *Cellulose* 24, 3555–3571. <https://doi.org/10.1007/s10570-017-1352-4>

400 Moongraksathum, B., Shang, J.-Y., Chen, Y.-W., 2018. Photocatalytic Antibacterial
401 Effectiveness of Cu-Doped TiO₂ Thin Film Prepared via the Peroxo Sol-Gel Method.
402 *Catalysts* 8, 352. <https://doi.org/10.3390/catal8090352>

403 Pakdel, E., Naebe, M., Kashi, S., Cai, Z., Xie, W., Yuen, A.C.Y., Montazer, M., Sun, L.,
404 Wang, X., 2020. Functional cotton fabric using hollow glass microspheres: Focus on
405 thermal insulation, flame retardancy, UV-protection and acoustic performance. *Prog.*
406 *Org. Coatings* 141, 105553. <https://doi.org/10.1016/j.porgcoat.2020.105553>

407 Pelaez, M., Nolan, N.T., Pillai, S.C., Seery, M.K., Falaras, P., Kontos, A.G., Dunlop, P.S.M.,
408 Hamilton, J.W.J., Byrne, J.A., O’Shea, K., Entezari, M.H., Dionysiou, D.D., 2012. A
409 review on the visible light active titanium dioxide photocatalysts for environmental
410 applications. *Appl. Catal. B Environ.* 125, 331–349.
411 <https://doi.org/10.1016/j.apcatb.2012.05.036>

412 Rao, A., Pundir, V.S., Tiwari, A., Padarthy, Y., Rao, N.V.M., Aich, S., Roy, B., 2018.
413 Investigating the effect of dopant type and concentration on TiO₂ powder
414 microstructure via rietveld analysis. *J. Phys. Chem. Solids* 113, 164–176.
415 <https://doi.org/10.1016/j.jpcs.2017.10.030>

416 Saad, S.R., Mahmed, N., Abdullah, M.M.A.B., Sandu, A.V., 2016. Self-Cleaning Technology
417 in Fabric: A Review. *IOP Conf. Ser. Mater. Sci. Eng.* 133, 012028.

418 <https://doi.org/10.1088/1757-899X/133/1/012028>

419 Sayilkan, F., Asiltürk, M., Sayilkan, H., Önal, Y., Akarsu, M., Arpaç, E., 2005.

420 Characterization of TiO₂ synthesized in alcohol by a sol-gel process: The effects of

421 annealing temperature and acid catalyst. *Turkish J. Chem.* 29, 697–706.

422 Shaban, M., Abdallah, S., Khalek, A.A., 2016. Characterization and photocatalytic properties

423 of cotton fibers modified with ZnO nanoparticles using sol–gel spin coating technique.

424 *Beni-Suef Univ. J. Basic Appl. Sci.* 5, 277–283.

425 <https://doi.org/10.1016/j.bjbas.2016.08.003>

426 Shan, A.Y., Ghazi, T.I.M., Rashid, S.A., 2010. Immobilisation of titanium dioxide onto

427 supporting materials in heterogeneous photocatalysis: A review. *Appl. Catal. A Gen.*

428 389, 1–8. <https://doi.org/10.1016/j.apcata.2010.08.053>

429 Singh, V., Rao, A., Tiwari, A., Yashwanth, P., Lal, M., Dubey, U., Aich, S., Roy, B., 2019.

430 Study on the effects of Cl and F doping in TiO₂ powder synthesized by a sol-gel route

431 for biomedical applications. *J. Phys. Chem. Solids* 134, 262–272.

432 <https://doi.org/10.1016/j.jpcs.2019.06.011>

433 Slavin, Y.N., Asnis, J., Häfeli, U.O., Bach, H., 2017. Metal nanoparticles: understanding the

434 mechanisms behind antibacterial activity. *J. Nanobiotechnology* 15, 65.

435 <https://doi.org/10.1186/s12951-017-0308-z>

436 Tahmasebiazad, N., Hamedani, M.T., Shaban Ghazani, M., Pazhuanfar, Y., 2020.

437 Photocatalytic activity and antibacterial behavior of TiO₂ coatings co-doped with copper

438 and nitrogen via sol–gel method. *J. Sol-Gel Sci. Technol.* 93, 570–578.

439 <https://doi.org/10.1007/s10971-019-05085-1>

440 Unwiset, P., Makdee, A., Chanapattharapol, K.C., Kidkhunthod, P., 2018. Effect of Cu

441 addition on TiO₂ surface properties and photocatalytic performance: X-ray Absorption
442 Spectroscopy analysis. *J. Phys. Chem. Solids* 120, 231–240.
443 <https://doi.org/10.1016/j.jpics.2018.05.003>

444 Yoong, L.S., Chong, F.K., Dutta, B.K., 2009. Development of copper-doped TiO₂
445 photocatalyst for hydrogen production under visible light. *Energy* 34, 1652–1661.
446 <https://doi.org/10.1016/j.energy.2009.07.024>

447 Zahid, M., Papadopoulou, E.L., Suarato, G., Binas, V.D., Kiriakidis, G., Gounaki, I., Moira,
448 O., Venieri, D., Bayer, I.S., Athanassiou, A., 2018. Fabrication of visible light-induced
449 antibacterial and self-cleaning cotton fabrics using manganese doped TiO₂ nanoparticles.
450 *ACS Appl. Bio Mater.* 1, 1154–1164. <https://doi.org/10.1021/acsabm.8b00357>

451 Zhang, G., Wang, D., Yan, J., Xiao, Y., Gu, W., Zang, C., 2019. Study on the Photocatalytic
452 and Antibacterial Properties of TiO₂ Nanoparticles-Coated Cotton Fabrics. *Materials*
453 (Basel). 12, 2010. <https://doi.org/10.3390/ma12122010>

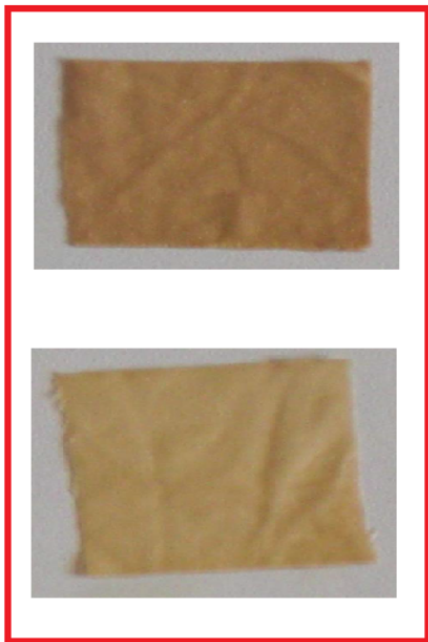
454 Zhu, J., Yang, J., Bian, Z.-F., Ren, J., Liu, Y.-M., Cao, Y., Li, H.-X., He, H.-Y., Fan, K.-N.,
455 2007. Nanocrystalline anatase TiO₂ photocatalysts prepared via a facile low temperature
456 nonhydrolytic sol–gel reaction of TiCl₄ and benzyl alcohol. *Appl. Catal. B Environ.* 76,
457 82–91. <https://doi.org/10.1016/j.apcatb.2007.05.017>

458

Raw cotton fabric



Stained cotton fabric



After 1hour illumination



After 2 hours illumination

